Journal of the Korean Society of Surveying, Geodesy, Photogrammetry and Cartography
Vol. 33, No. 6, 557-567, 2015
http://dx.doi.org/10.7848/ksgpc.2015.33.6.557

ISSN 1598-4850(Print)
ISSN 2288-260X(Online)
Original article

# Accuracy Comparison Between Image-based 3D Reconstruction Technique and Terrestrial LiDAR for As-built BIM of Outdoor Structures

Lee, Jisang[1] · Hong, Seunghwan[2] · Cho, Hanjin[3] · Park, Ilsuk[4]
Cho, Hyoungsig[5] · Sohn, Hong-Gyoo[6]

**Abstract**

With the increasing demands of 3D spatial information in urban environment, the importance of point clouds generation techniques have been increased. In particular, for as-built BIM, the point clouds with the high accuracy and density is required to describe the detail information of building components. Since the terrestrial LiDAR has high performance in terms of accuracy and point density, it has been widely used for as-built 3D modelling. However, the high cost of devices is obstacle for general uses, and the image-based 3D reconstruction technique is being a new attraction as an alternative solution. This paper compares the image-based 3D reconstruction technique and the terrestrial LiDAR in point of establishing the as-built BIM of outdoor structures. The point clouds generated from the image-based 3D reconstruction technique could roughly present the 3D shape of a building, but could not precisely express detail information, such as windows, doors and a roof of building. There were 13.2~28.9 cm of RMSE between the terrestrial LiDAR scanning data and the point clouds, which generated from smartphone and DSLR camera images. In conclusion, the results demonstrate that the image-based 3D reconstruction can be used in drawing building footprint and wireframe, and the terrestrial LiDAR is suitable for detail 3D outdoor modeling.

Keywords : Terrestrial LiDAR, Image-based 3D Reconstruction, Building Information Modelling (BIM), point clouds, Structure from Motion (SfM)

## 1. Introduction

Recently, 3D spatial information is becoming necessary in various fields, such as robotics, disaster management, and Information and Communication Technology (ICT). Moreover, those developments in smartphones and telecommunication environments have accelerated the utilization of 3D spatial information. In particular, there are increasing demands for accurate and precise construction of 3D spatial information in the Building Information Modelling (BIM) field in order to measure, inspect, and verify the safety of structures (Randall, 2011; Isikdag *et al*., 2013). However, the acquisition of accurate and precise 3D spatial data is a laborious and costly task. For the reason, researchers currently perform studies in developing more efficient techniques in cost and time.

Received 2015. 11. 30, Revised 2015. 12. 24, Accepted 2015. 12. 31
1) School of Civil and Environmental Engineering, Yonsei University, Seoul 03722, Korea (E-mail: ontheground@yonsei.ac.kr)
2) Member, School of Civil and Environmental Engineering, Yonsei University, Seoul 03722, Korea (E-mail: hotaeim@yonsei.ac.kr)
3) School of Civil and Environmental Engineering, Yonsei University, Seoul 03722, Korea (E-mail: xkwks4568@yonsei.ac.kr)
4) School of Civil and Environmental Engineering, Yonsei University, Seoul 03722, Korea (E-mail: moncher@yonsei.ac.kr)
5) Member, School of Civil and Environmental Engineering, Yonsei University, Seoul 03722, Korea (E-mail: f15kdaum@yonsei.ac.kr)
6) Corresponding Author, Member, School of Civil and Environmental Engineering, Yonsei University, Seoul 03722, Korea (E-mail: sohn1@yonsei.ac.kr)

Those acquisition methods for 3D data can be classified into two major categories; one is the range-based technique using a Light Detecting and Ranging (LiDAR), while the other is image-based 3D reconstruction techniques based on the principle of the photogrammetry and computer vision (Tang *et al*., 2010; Klein *et al*., 2012). The terrestrial LiDAR collects the 3D data of target objects by bouncing light off from the object and contours an image on the basis of light-return rates and angles. The terrestrial LiDAR has been verified as the most superior solution for 3D data acquisition in terms of getting accurate and dense point data in relatively short time (Jazayeri *et al*., 2014; Cho *et al*., 2015). The terrestrial LiDAR has been utilized to acquire accurate 3D point clouds data in various fields, such as construction management (Su *et al*., 2006), forest science (Dassot *et al*., 2011), landslide monitoring (Jones, 2006), and snow depth measurement (Prokop, 2008). The point clouds observed by terrestrial LiDAR have been specifically applied in the field of BIM to improve the efficiency for facility management of indoor and outdoor environments (Tang *et al*., 2010; Jung *et al*., 2014; Hong *et al*., 2015). Randall (2011) conceptually proposed standards for building information modelling based on point clouds, gathered from the LiDAR. According to the propose, the point clouds for structural analysis and inspection needs 1cm of accuracy, while it needs 1m of accuracy for rapid urban modelling. However, in the study, an actual test had not been conducted, whereas there was also no well-defined evaluation standard yet for evaluating the performance of 3D BIM construction.

Despite of its accuracy and productivity, the terrestrial LiDAR device accompanies a financially big concern for general uses due to its expensive costs, more than a hundred thousand dollars. An alternative solution to reduce the cost of point clouds acquisition is the image-based 3D reconstruction techniques, which have been already applied in some commercial fields via image big data collected from the internet (Snavely *et al*., 2007; Uricchio, 2011). The Image-based 3D reconstruction techniques, which can be conducted automatically with a relatively low cost, have been studied for various applications, such as construction sites (Golparvar-Fard *et al*., 2011), facility management (Bhatla *et al*., 2012), and archaeology (Brutto and Meli, 2012; Kersten and Lindstaedt, 2012; De Reu *et al*., 2013).

However, when using multiple image data from uncertain sources, the quality of final products could be negatively affected by the inconsistency in captured date, weather conditions, resolution, as well as the ambiguity of image geometry. Due to the qualitative uncertainty of 3D point clouds generated from multiple sources, a qualitative analysis evaluating the performance of the image-based 3D reconstruction techniques has been conducted. In fact, the results were cross analyzed with the observed data from traditional measuring method (Dai and Lu, 2010) and terrestrial LiDAR data (Dai *et al*., 2013). In addition, Bhatla (2012) conducted the image-based as-built 3D modeling of bridge, which compared with the 3D model generated from 2D drawings, and Yang *et al*. (2013) applied the image-based 3D reconstruction to an augmented reality technique.

Previous studies had verified the performance of image-based 3D reconstruction technique for various applications. For as-built BIM, accuracy and point density of a point clouds must be achieved in centimeter level to express the detail geometric information of building structures. Since the distance between target and camera sensor was not close in outdoor observation, those point clouds from multiple images cannot ensure their point density and accuracy without special platforms, such as an unmanned areal vehicle (UAV) (Dai *et al*., 2013).

In this regard, this paper has conducted the evaluation of image-based 3D reconstruction technique and terrestrial LiDAR, in terms of establishing as-built BIM of outdoor structures. Also, their performances were compared with respect to noise ratio, point density, and accuracy. Images for generating a point clouds were collected by smartphone camera and Digital Single-Lens Reflex (DSLR) camera, which can be easily used by general users with the low cost. A terrestrial LiDAR device of pulsed type, which is widely used for outdoor observation, was selected. For the comparison analysis, the coordinate system of point clouds from multiple images was converted into the coordinate system of the LiDAR data, using 3D conformal

transformation and Iterative Closest Point (ICP) algorithm. For the accuracy comparison, those checking points were extracted by the RANdom SAmple Consensus (RANSAC) algorithm.

## 2. Methodology

In the paper, the image-based 3D reconstruction method and the terrestrial LiDAR scannning for 3D modelling of outdoor building were conducted independently and compared in terms of the point density and accuracy. The overall process is summarized in Fig. 1.

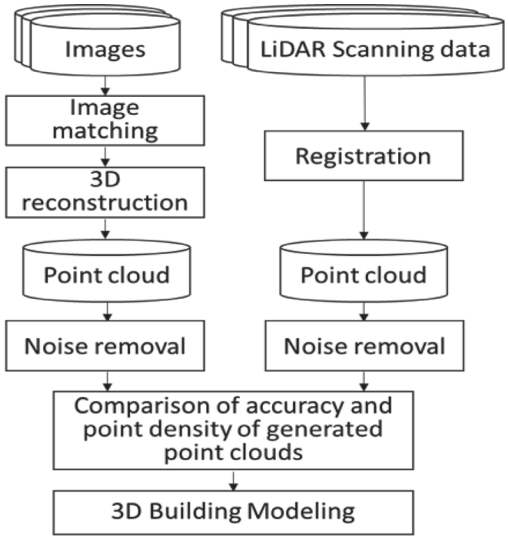


**Fig. 1. Flowchart of overall process**

### 2.1 Test site and device

In comparing the image-based 3D reconstruction technique and the terrestrial LiDAR scanning for outdoor modelling, the outdoor building image of size is 50 m x 15 m x 35 m was selected. The test building presents in the Fig.2, including front door with stair, windows, roof, and many other building components, which are generally considered as structures in outdoor building modelling.

The Leica ScanStation 2 was used for the LiDAR scanning and its specification was summarized in Table 1 (Leica Geosystems, 2007). As shown in Table 1, the Leica ScanStation 2, which is the pulsed type scanner, has an

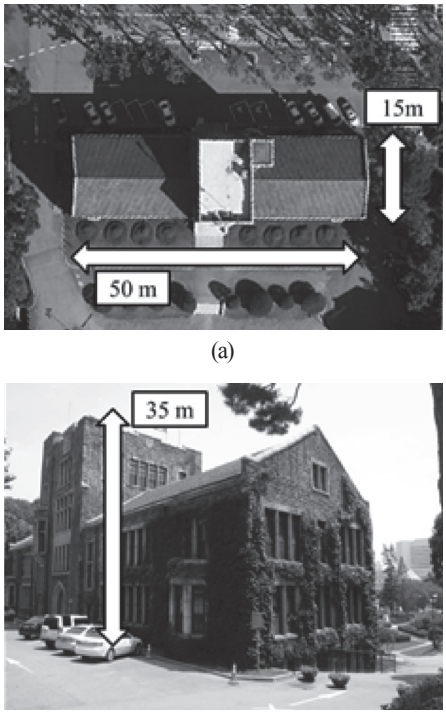


**Fig. 2. Test site for 3D outdoor modelling: (a) top view, and (b) side view**

effective range of 300 m and positioning accuracy of 6 mm.

A smartphone camera and a DSLR camera were used

**Table 1. Specification of Leica Scanstation 2**

| Type | | Pulsed |
|---|---|---|
| Range | | 300m@90%, 134m@18% albedo |
| Scan rate | | Up to 50,000 points/sec |
| Accuracy of single measurement* | Position* | 6mm |
| | Distance* | 4mm |
| | Angle | 60μrad |
| Field of view | Horizontal | 360° (maximum) |
| | Vertical | 270° (maximum) |
| Weight | | 18.5 kg |
| Size (depth, width, height) | | 265, 370, 510 mm |
| Camera | | Integrated high-resolution digital camera |

* At 1 m∼50 m range, one sigma

**Table 2. Specification of the utilized smartphone and DSLR cameras**

| Specification | Smartphone camera | DSLR camera |
|---|---|---|
| Model | Samsung Galaxy S II | Canon EOS Rebel T3i |
| Sensor type | CMOS | CMOS |
| Sensor format | 1/3.2″ | APS-C |
| Sensor size | 4.54mm × 3.42mm | 22.30mm × 14.90mm |
| Pixel Pitch | 1.39 μm | 4.30 μm |
| Focus mode | Autofocus | Autofocus |
| Image size | 3264 × 2448 | 5184 × 3456 |
| Focal length | 4 mm | 17 mm |

to evaluate the performance of the image-based 3D reconstruction technique. The Table 2 shows the specification of the smartphone and the DSLR camera, which are used in the experiments. As shown in Table 2, the spatial resolutions of the smartphone images were lower than those of the DSLR images.

## 2.2 Terrestrial LiDAR scanning

Since the single-scanned data cannot cover every side of the building, the multiple scanning process and registration process to convert the relative coordinate systems of the multi-scanned data to a common coordinate system are required. The registration can be classified into the target-free method and the target-based method. The target-free method based on the ICP algorithm can automatically perform the registration, but the accuracy cannot be guaranteed. Thus, the target-based method using artifacts, such as sphere, paddle, and paper targets and natural point features is generally applied for as-built BIM due to its accuracy and efficiency. In this study, natural point features in overlapped areas were manually extracted and used for the target-based registration. In addition, target-free method was applied to improve precision of registration.

A model for the registration of point clouds with an absolute scale factor can be conducted on the basis of 3D rigid body transformation, which includes a rotation matrix ( $M_{\omega\phi\kappa}$ ),and translation vector ( $[X_T, Y_T, Z_T]^T$ ). The model equation can be represented by Eq. (1):

$$\begin{bmatrix} X_g \\ Y_g \\ Z_g \end{bmatrix} = M_{\omega\phi\kappa} \begin{bmatrix} X_{obs} \\ Y_{obs} \\ Z_{obs} \end{bmatrix} + \begin{bmatrix} X_T \\ Y_T \\ Z_T \end{bmatrix} \tag{1}$$

where $X_g$, $Y_g$ and $Z_g$ are the 3D coordinates of the converted points, $X_{obs}$, $Y_{obs}$ and $Z_{obs}$ are the original 3D coordinates of the observed points, and is the rotation matrix. This can be calculated as follows:

$$\begin{aligned} & M_{\omega\phi\kappa} = M_\kappa M_\phi M_\omega \\ & where,\ M_\omega = \begin{bmatrix} 1 & 0 & 0 \\ 0 & \cos\omega & \sin\omega \\ 0 & -\sin\omega & \cos\omega \end{bmatrix}, M_\phi = \begin{bmatrix} \cos\phi & 0 & -\sin\phi \\ 0 & 1 & 0 \\ \sin\phi & 0 & \cos\phi \end{bmatrix}, \\ & M_\kappa = \begin{bmatrix} \cos\kappa & -\sin\kappa & 0 \\ \sin\kappa & \cos\kappa & 0 \\ 0 & 0 & 1 \end{bmatrix} \end{aligned} \tag{2}$$

where, $\omega$, $\phi$ and $\kappa$ are the rotation angles about X-axis, Y-axis, and Z-axis, respectively.

The 3D rigid body transformation requires at least two matching points to estimate the six transformation parameters. However, it is difficult to extract the accurate 3D coordinates of common point features in overlapped point clouds. To overcome the locational ambiguity of matching points, the ICP algorithm can be additionally applied for a robust registration. The ICP algorithm iteratively finds the closest points in a pair of point clouds and automatically estimates transformation parameters for the minimization of locational inconsistency between a pair of point clouds (Besl and McKay, 1992). After the target-based registration using the point features is conducted, the ICP algorithm can be additionally conducted to improve precision of the aligned point clouds.

## 2.3 Image-based 3D reconstruction

The Structure-from-Motion (SfM) technique-based on the integration of the principle of photogrammetry and computer vision- is known as the most practical solution to generate a point cloud from hundreds or thousands of images of which camera parameters and orientations are unknown (Golparvar-Fard *et al*., 2011; Brutto and Meli, 2012). Since the interior orientation parameters of a focal length and lens distortion are estimated relatively in the SfM process, the process for estimating camera parameters distortions can be omitted (Golparvar-Fard *et al*., 2011).

The flowchart of image-based 3D reconstruction is

represented in Fig. 3 (Snavely *et al*., 2006). To generate point clouds from multiple image sets, feature points must be extracted and conjugate point sets are determined from the feature points. To extract featured points for generating point clouds, those keypoint detection and matching procedures were conducted on the basis of the Scale Invariant Feature Transform (SIFT) algorithm. By the SIFT algorithm, the featured points in each image are extracted automatically as SIFT keypoints (Lowe, 2004). The correspondence between the SIFT keypoints is calculated and matched based on the nearest neighborhood matching scheme and the RANSAC algorithm. Then, conjugate point sets are determined and utilized to relatively estimate the camera parameters, such as the focal length, lens distortions, location, and view angle. At first, the camera parameters of a single pair of images having a large number of conjugate points and long baseline are estimated; then, the camera parameters of additional cameras were initialized based on direct linear transformation (DLT) with RANSAC scheme to avoid getting stuck in the bad local minima (Hartley and Zisserman, 2003); Lastly, the initialized parameters were optimized based on bundle adjustment and point clouds following to the process (Lourakis and Argyros, 2004).

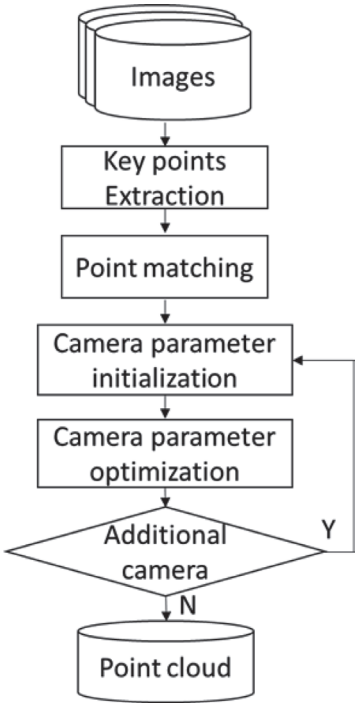


**Fig. 3. Flowchart of image-based 3D reconstruction**

Software based on the SfM process has been developed as an open source software, commercial packages and web-based services (Bartoš *et al*., 2014). In particular, the Photosynth - a web-based free software provided by Microsoft - has been utilized to acquire 3D point clouds data for various researches (Snavely *et al*., 2006; Dowling *et al*., 2009; Pomaska, 2009; Hwang *et al*., 2012; Microsoft, 2015). In the study, we applied Microsoft's Photosynth for the image-based 3D reconstruction technique. By the program, the SfM process was conducted automatically, so as point clouds were generated from multiple image sets capturing targets.

## 2.4 Accuracy assessment

For accuracy assessment of the image-based 3D reconstruction technique, it is necessary to perform a registration process converting coordinate system of generated point clouds into the common coordinate system. Unlike the registration process between sets of terrestrial LiDAR scanning data, the point clouds from the image-based 3D reconstruction technique had a relative scale factor and coordinate system. Therefore, the registration process to convert coordinate systems of point clouds sets into common coordinate system with an absolute scale was conducted based on the 3D conformal transformation, which includes scale parameter ($\lambda$), rotation matrix, and translation vector. To estimate the scale, rotation and translation parameters, the five matching points are required at least. The equation of 3D conformal transformation can be represented by Eq. (3):

$$\begin{bmatrix} X_g \\ Y_g \\ Z_g \end{bmatrix} = \lambda R_{\omega\phi\kappa} \begin{bmatrix} X_{obs} \\ Y_{obs} \\ Z_{obs} \end{bmatrix} + \begin{bmatrix} X_T \\ Y_T \\ Z_T \end{bmatrix} \tag{3}$$

In this paper, the registration process, based on the 3D conformal transformation, and the ICP algorithm was conducted sequentially. Since we could acquire precise point clouds having an actual scale with the terrestrial LiDAR, the point clouds generated by the image-based 3D reconstruction techniques were converted into the coordinate system of the LiDAR data. The 3D conformal transformation was

conducted using manually selected matching points, as the estimated parameters were used as the initial values for the ICP algorithm. Since the accuracy of the ICP algorithm can be affected by noise points in point clouds, we checked the effect of noise points on the accuracy of the ICP algorithm to merge a pair of point clouds from difference sources.

After the registration of the point clouds sets, an accuracy assessment was conducted using the intersection points of main wall components of the test building. RANSAC, proposed by Fischler and Bolles (1981), was applied to estimate plane model parameters from the observed point clouds including noises. To find the best plane model of the point clouds data, the RANSAC algorithm randomly selects the sample points to estimate the candidate planes and check a number of points including in the plane models. A model equation of the plane inside the RANSAC algorithm can be defined by Eq. (4):

$$ax + by + cz + d = 0 \tag{4}$$

where, $a$, $b$, $c$ and $d$ are the parameters of the plane model, $x$, $y$ and $z$ are the 3D coordinates of a point. Since the parameters of the plane model are dependent, constraints listed in Eq. (5) and Eq. (6) are required.

$$a^2 + b^2 + c^2 = 1 \tag{5}$$

$$a \geq 0 \tag{6}$$

The main plane components extracted from each point clouds were used to calculate intersection points for the accuracy assessment. The Fig. 4 describes the intersection of planes. As shown in Fig. 4, three plane components can determine a intersection point.

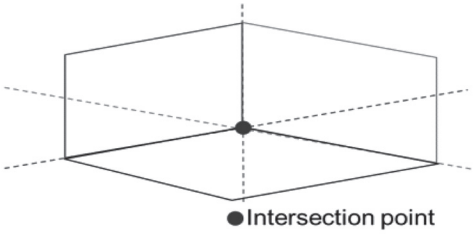


**Fig. 4. Relationship between planes and intersection points**

In this paper, since the image-based 3D reconstruction techniques cannot guarantee the accuracy of point clouds, the accuracy assessments of were conducted based on the terrestrial LiDAR data as ground truth. For the accuracy comparison, those wall components in generated point clouds were extracted based on the RANSAC scheme, while intersection points were determined from the extracted planar wall models. By RANSAC algorithm, the main wall components in point clouds could be extracted automatically, when the extracted wall components were labelled manually.

## 3. Experiments and Results

### 3.1 Results of terrestrial LiDAR scanning

To cover every side of the test building, terrestrial LiDAR scans were conducted five times. The point clouds density

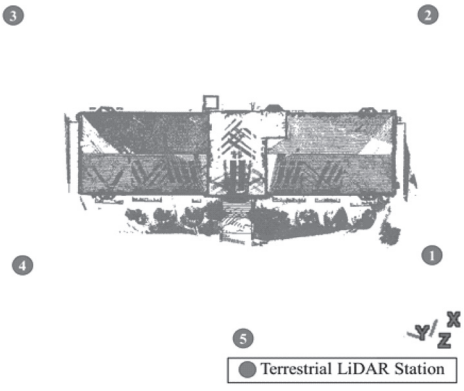


**Fig. 5. Location of terrestrial LiDAR stations for scanning**

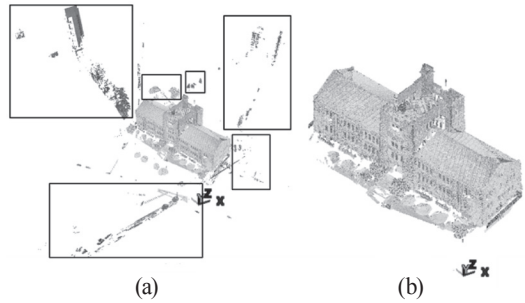


**Fig. 6. Point clouds observed by a terrestrial LiDAR: (a) original point clouds (box: noisy information such as adjacent buildings, cars, people and trees; number of noise points: 222,834), and (b) remaining noise-removed point clouds (number of points: 3,999,133)**

was about 1 cm at 10 m from the LiDAR and the distances between the LiDAR, and the target were from 20 m to 30 m. The Fig. 5 illuminates the location of Terrestrial LiDAR station for scanning.

A total number of 4,221,967 points were acquired and 222,834 points - such as adjacent buildings, cars, people, and trees - were removed as noisy information. A Fig. 6 illuminates the original point clouds and noise-removed point clouds. As shown in the Fig. 6, although the incidence angles of laser beam on roofs were steep, point clouds was clearly presented.

### 3.2 Results of the image-based 3D reconstruction

Both the smartphones and the DSLR cameras captured 400 images of the test building, respectively. The image collection was conducted from various angles and locations to ensure sufficient geometric data for generating point clouds. A Fig. 7. represents the geometry of used images and generated point clouds from multiple images. As shown in Fig. 7, the images were configured in relative coordinate system and generated a point clouds.

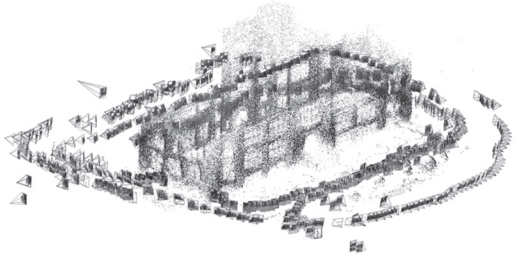

**Fig. 7. Geometry of images used for point clouds generation**

Each image set obtained using the smartphones and the DSLR camera was respectively used for point clouds generation. In addition, the point clouds was generated using all of the collected images by both camera sensors. The Fig. 8 represents the point clouds created by the image-based 3D reconstruction technique. As shown in Fig. 8, the point clouds, which were generated by the image-based reconstruction technique, could roughly represent an as-built building in an outdoor environment.

The number of points created from the smartphone and the DSLR camera images were 635,140, 226,060, and 857,344 points, in order. The point clouds achieved from the camera images were much sparser than those observed by the terrestrial LiDAR. Not only that, the roof components of the building could not be represented in point clouds form because of the repetitive roof pattern, steep view angle, and low spatial resolution of the terrestrial camera images.

The point clouds created from the smartphone images, the DSLR camera images, and the entire images had 24.7 %, 13.6 % and 11.1 % of the noise points, respectively. The point clouds created from the smartphone images had more noises and lower precision than the other point clouds. The point clouds created from the entire images, which had different spatial resolutions and geometry, had the most detail information.

As shown in Fig. 9, comparing to the LiDAR scanning data, the point clouds created by the image-based 3D reconstruction technique had much more noisy points near the wall and could not express the detail information such as

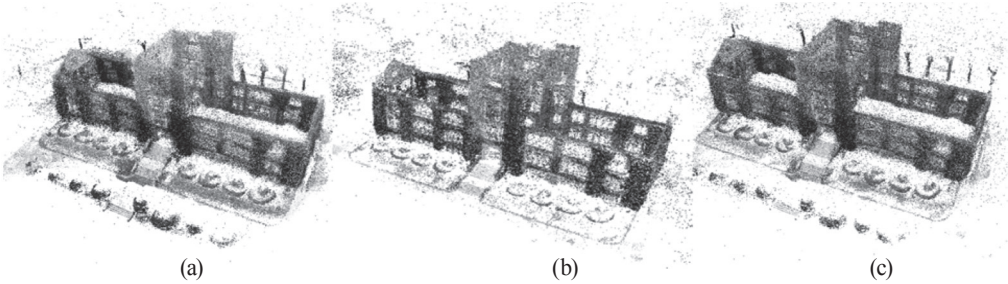

(a) (b) (c)

**Fig. 8. The point clouds achieved by the image-based 3D reconstruction technique: (a) using smartphone camera (number of images: 400 / number of points: 635,140 / number of noise points: 157,359), (b) using DSLR camera (number of images: 400 / number of points: 226,060 / number of noise points: 30,645), and (c) using smartphone and DSLR cameras (number of images: 800 / number of points: 857,344 / number of noise points: 95,402)**

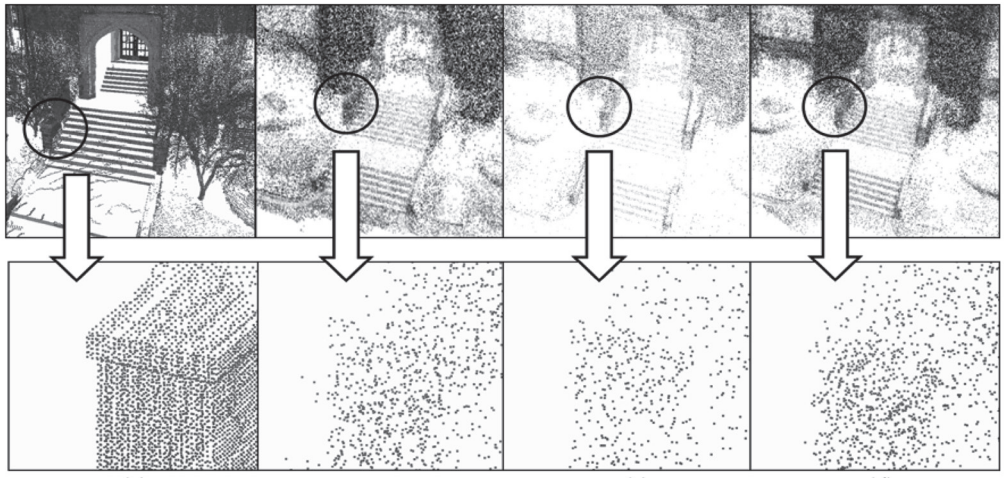


**Fig. 9. Expressiveness of the point clouds achieved by LiDAR and camera images: (a) using LiDAR, (b) using smartphone camera images, and (c) using DSLR camera images (d) using smartphone and DSLR cameras images**

windows, stairs, and doors in high level 3D outdoor modeling. Despite of its financial merit for the general users, the point clouds generated from multiple images were insufficient for as-built 3D modeling of outdoor buildings.

### 3.3 Results of the accuracy assessment

For the accuracy assessment, the main wall planes of a test building were estimated from each point clouds based on the RANSAC algorithm. Since the roof components in the point clouds achieved from camera images, however, could not be extracted because of its low point density. The accuracy assessment of image-based 3D reconstruction technique was conducted on the 2D horizontal coordinate system. Each plane was projected on the XY plane and the

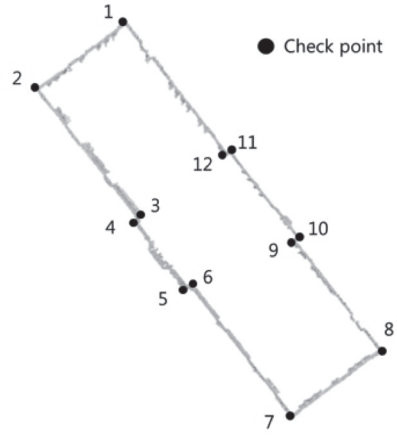


**Fig. 10. LiDAR scanning data projected on the XY plane and the location and label of check points for accuracy assessment**

**Table 3. Result of accuracy assessment: (Case #1) applying the 3D conformal transformation, (Case #2) applying the 3D conformal transformation and ICP algorithm with raw point clouds generated from multiple images, and (Case #3) applying the 3D conformal transformation, ICP algorithm with noise-removed point clouds**

| Sensor | RMSE (cm) | | | Mean error (cm) | | | Std. dev. of error (cm) | | |
|---|---|---|---|---|---|---|---|---|---|
| | Case#1 | Case#2 | Case#3 | Case#1 | Case#2 | Case#3 | Case#1 | Case#2 | Case#3 |
| Smart phone | 28.61 | 25.94 | 28.91 | 25.61 | 22.86 | 26.24 | 13.32 | 12.80 | 12.68 |
| DSLR | 23.69 | 27.58 | 24.93 | 22.89 | 26.02 | 23.77 | 6.35 | 9.55 | 7.86 |
| Smart phone and DSLR | 18.23 | 13.93 | 13.23 | 14.99 | 10.03 | 9.14 | 10.83 | 10.09 | 9.98 |

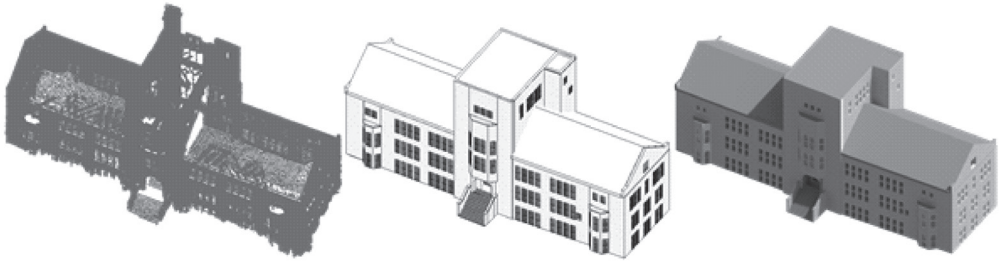

(a) (b) (c)

**Fig. 11. Result of the 3D modeling: (a) point clouds, (b) Geometric model, and (c) Rendered model**

twelve intersection points between the projected planes were extracted as the check points for quantitative accuracy assessment. A Fig. 10 presents point clouds projected on the XY plane and the labels of check points.

The Table 3 shows the locational inconsistency of check points. The RMSE of image-based 3D reconstruction was in the range from 13.2 cm to 28.9 cm depending on the types of the images and registration methods. The ICP algorithm could improve the accuracy of registration for the precise point sets from the entire images or DSLR images. However, the ICP algorithm may reduce the accuracy of registration if the point clouds contain many noise points like those, created by the smartphone images. When the initial parameters for the ICP algorithm were determined without the initial estimation of the parameters - like scale, rotation, and translation, the ICP algorithm did not work due to the existence of widespread noise.

### 3.4 3D outdoor modeling

Because of the insufficient accuracy and precision of the point clouds from the image-based 3D reconstruction technique, the terrestrial LiDAR scanning data was utilized for the as-built BIM in this research. The as-built BIM of an outdoor building was conducted using Autodesk's Revit 2015 software (Autodesk, 2015), while Fig. 11 describes the model created on the basis of the LiDAR scanning data. As shown in Fig. 11, the roof, windows, stairs, and door components of testing building could be expressed by the terrestrial LiDAR data.

## 4. Conclusions

The study has compared the accuracy and the point density of the point clouds created from the image-based 3D reconstruction technique and the terrestrial LiDAR scanning data for as-built BIM of outdoor structures. Based on the outdoor experiment, the following conclusions were drawn:

1. The image-based 3D reconstruction technique could obtain the rough shape of an outdoor building. There were 13.2∼28.9 cm of RMSE between the point clouds generated from multiple images and the LiDAR scanning data.
2. The resolution and the geometry of the captured images had an impact on the accuracy and the precision of point clouds created, via the image-based 3D reconstruction technique. The point clouds generated from the smartphone images had the largest number of noise with the lowest accuracy.
3. The point clouds created from multiple images had numerous noise points that could not represent detail 3D information compared to the terrestrial LiDAR scanning data. However, the image-based 3D reconstruction techniques could not be the practical solution for the as-built BIM. For as-built BIM, those point clouds with centimeter level of accuracy and point density were necessary to represent the detail information of building components - such as door, window, wall, and roof.

Although the image-based 3D reconstruction technique holds potentials for as-built 3D urban modeling, there were problems that generated point clouds had relative scale, insufficient accuracy, and numerous noise points. Regarding to it, we could conclude that the terrestrial LiDAR is still the most practical solution for as-built 3D BIM construction. In the future study, our research team will plan to develop the

noise filtering and the accuracy improving algorithms for the image-based 3D reconstruction. In addition, we expect a new techniques based on image big data to be developed as solutions for improving data quality.

## Acknowledgments

This work was supported by the Technology Development Project of Private and Public Joint Investment [Project Number : S2287109] funded by the Small and Medium Business Administration (SMBA, Korea).

## References

Autodesk (2015), Revit, *Autodesk*, California, http://www.autodesk.com/products/revit-family/overview (last date accessed: 31 January 2015).

Bartoš, K., Pukanská, K., and Sabová, J. (2014), Overview of available open-source photogrammetric software, its use and analysis, *International Journal for Innovation Education and Research*, Vol. 2, No. 4, pp. 62-70.

Besl, P.J. and McKay, N.D. (1992), A method for registration of 3-D shapes, *SPIE 1611, Sensor Fusion IV: Control Paradigms and Data Structures, 586*, International Society for Optics and Photonics, 30 April, Boston, MA, pp. 586-606.

Bhatla, A., Choe, S.Y., Fierro, O., and Leite, F. (2012), Evaluation of accuracy of as-built 3D modeling from photos taken by handheld digital cameras, *Automation in Construction*, Vol. 28, pp. 116-127.

Brutto, M.L. and Meli, P. (2012), Computer vision tools for 3D modelling in archaeology, *International Journal of Heritage in the Digital Era*, Vol. 1, pp. 1-6.

Cho, H., Hong, S., Kim, S., Park, H., Park, I., and Sohn, H.-G. (2015), Application of a terrestrial LIDAR system for elevation mapping in Terra Nova Bay, Antarctica, *Sensors*, Vol. 15, No. 9, pp. 23514-23535.

Dai, F. and Lu, M. (2010), Assessing the accuracy of applying photogrammetry to take geometric measurements on building products, *Journal of Construction Engineering and Management*, Vol. 136, No. 2, pp. 242-250.

Dai, F., Rashidi, A., Brilakis, I., and Vela, P. (2013), Comparison of image-based and time-of-flight-based technologies for three-dimensional reconstruction of infrastructure, *Journal of Construction Engineering and Management*, Vol. 139, No. 1, pp. 69-79.

Dassot, M., Constant, T., and Fournier, M. (2011), The use of terrestrial LiDAR technology in forest science: application fields, benefits and challenges, *Annals of Forest Science*, Vol. 68, No. 5, pp. 959-974.

De Reu, J., Plets, G., Verhoeven, G., De Smedt, P., Bats, M., Cherretté, B., De Maeyer, W., Deconynck, J., Herremans, D., and Laloo, P. (2013), Towards a three-dimensional cost-effective registration of the archaeological heritage, *Journal of Archaeological Science*, Vol. 40, No. 2, pp. 1108-1121.

Dowling, T., Read, A., and Gallant, J. (2009), Very high resolution DEM acquisition at low cost using a digital camera and free software, *Proceedings of 18th World IMACS/MODSIM International Congress on Modelling and Simulation*, 13–17 July, Australia, pp. 2479-2485.

Fischler, M.A. and Bolles, R.C. (1981), Random sample consensus: a paradigm for model fitting with applications to image analysis and automated cartography, *Communications of the ACM*, Vol. 24, No. 6, pp. 381-395.

Golparvar-Fard, M., Bohn, J., Teizer, J., Savarese, S., and Peña-Mora, F. (2011), Evaluation of image-based modeling and laser scanning accuracy for emerging automated performance monitoring techniques, *Automation in Construction*, Vol. 20, No. 8, pp. 1143-1155.

Hartley, R. and Zisserman, A. (2003), *Multiple View Geometry in Computer Vision*, Cambridge University Press, Cambridge.

Hong, S.H., Cho, H.S., Kim, N.H., and Sohn, H.G. (2015), 3D indoor modeling based on terrestrial laser scanning, *Journal of the Korean Society of Civil Engineers*, Vol. 35, No. 2, pp. 525-531. (in Korean with English abstract)

Hwang, J.T., Weng, J.S., and Tsai, Y.T. (2012), 3D modeling and accuracy assessment-a case study of photosynth, *20th International Conference on Geoinformatics,* Geoinformatics, 15-17 June, Hong Kong, pp. 1-6.

Isikdag, U., Zlatanova, S., and Underwood, J. (2013), A BIM-oriented model for supporting indoor navigation

requirements, *Computers*, *Environment and Urban Systems*, Vol. 41, pp. 112-123.

Jazayeri, I., Rajabifard, A., and Kalantari, M. (2014), A geometric and semantic evaluation of 3D data sourcing methods for land and property information, *Land Use Policy*, Vol. 36, pp. 219-230.

Jones, L. (2006), Monitoring landslides in hazardous terrain using terrestrial LiDAR: an example from Montserrat, *Quarterly Journal of Engineering Geology and Hydrogeology*, Vol. 39, No. 4, pp. 371-373.

Jung, J., Hong, S., Jeong, S., Kim, S., Cho, H., Hong, S., and Heo, J. (2014), Productive modeling for development of as-built BIM of existing indoor structures, *Automation in Construction*, Vol. 42, pp. 68-77.

Kersten, T.P. and Lindstaedt, M. (2012), Image-based low-cost systems for automatic 3D recording and modelling of archaeological finds and objects, In: Marinos I., Dieter F., Johanna L., Rob D., Fabio R., and Rossella C. (eds.), *Progress in Cultural Heritage Preservation*, Springer Berlin Heidelberg, Hamburg, Germany, pp. 1-10.

Klein, L., Li, N. and Becerik-Gerber, B. (2012), Imaged-based verification of as-built documentation of operational buildings, *Automation in Construction*, Vol. 21, pp. 161-171.

Leica Geosystems (2007), Datasheet of Leica ScanStation 2, *Leica Geosystems*, Switzerland, http://hds.leica-geosystems.com (last date accessed: 31 January 2015).

Lourakis, M. and Argyros, A. (2004), The design and implementation of a generic sparse bundle adjustment software package based on the levenberg-marquardt algorithm, *Technical Report 340*, Institute of Computer Science-FORTH, Heraklion, Crete, Greece, Vol. 1, No. 2, p. 5.

Lowe, D.G. (2004), Distinctive image features from scale-invariant keypoints, *International Journal of Computer Vision*, Vol. 60, No. 2, pp. 91-110.

Microsoft (2008), Photosynth, *Microsoft*, Washington, https://photosynth.net (last date accessed: 31 January 2015).

Pomaska, G. (2009), Utilization of photosynth point clouds for 3D object reconstruction. *Proceedings of the 22nd CIPA symposium*, International Committee for Documentation of Cultural Heritage, 11-15 October, Kyoto, Japan, p. 5.

Prokop, A. (2008), Assessing the applicability of terrestrial laser scanning for spatial snow depth measurements, *Cold Regions Science and Technology*, Vol. 54, No. 3, pp. 155-163.

Randall, T. (2011), Construction engineering requirements for integrating laser scanning technology and building information modeling, *Journal of Construction Engineering and Management*, Vol. 137, No. 10, pp. 797-805.

Snavely, N., Seitz, S. M., and Szeliski, R. (2006), Photo tourism: exploring photo collections in 3D. *ACM Transactions on Graphics (TOG)*, Vol. 25, No. 3, pp. 835-846.

Snavely, N., Seitz, S.M., and Szeliski, R. (2007), Modeling the world from internet photo collections, *International Journal of Computer Vision*, Vol. 80, No. 2, pp. 189-210.

Su, Y., Hashash, Y. and Liu, L. (2006), Integration of construction as-built data via laser scanning with geotechnical monitoring of urban excavation, *Journal of Construction Engineering and Management*, Vol. 132, No. 12, pp. 1234-1241.

Tang, P., Huber, D., Akinci, B., Lipman, R., and Lytle, A. (2010), Automatic reconstruction of as-built building information models from laser-scanned point clouds: A review of related techniques, *Automation in Construction*, Vol. 19, No. 7, pp. 829-843.

Uricchio, W. (2011), The algorithmic turn: photosynth, augmented reality and the changing implications of the image, *Visual Studies*, Vol. 26, No. 1, pp. 25-35.

Yang, M.D., Chao, C.F., Huang, K.S., Lu, L.Y., and Chen, Y.P. (2013), Image-based 3D scene reconstruction and exploration in augmented reality, *Automation in Construction*, Vol. 33, pp. 48-60.